Study on Evolution of Mining-induced Crack of Rock Mass Considering Hydromechanical Coupling Effects Based on Stabilized Nano CT Scan

Feng, Feisheng; Du, Wenfeng; Peng, Suping; Xing, Zhen-guo

State Key Laboratory of Coal Resources and Safe Mining, China University of Mining and Technology,Beijing, 100011

Abstract Rocks have different fracture development mechanisms under different circumstances with or without pressure, and under different triaxial confining pressure functions. it is important to research the influence between the development process of internal crack and external factors including different tectonic stress, different water pressure, different pressure rate and so on,realize the randomness and Non – random of crack development, and research the specific development mechanism of crack under a single impact factor.

Key words stabilized Nano CT scan, Mining-induced Crack, Hydromechanical Coupling Effects, maximum major stress

Introduction

In most rock engineering projects, crustal rocks stay in geological environments with fully coupled stress, flow, temperature, and chemical fields for long. In mining and slope engineering projects, the coupling between flow and stress fields is the primary factor controlling the behavior of rock masses. For example, stress field variations can change fractures in a rock mass, such as deformation and growth of pores and fractures, and thereby alter rock permeability and the state of water flow through the rock mass. Meanwhile, changes in fractures can drive the water within them to in turn affect their evolution(Zhang Youtian et al. 2005).The interaction between a rock mass and the water flow in it is referred to as flow-stress coupling.

Rock damage and failure resulting from artificially induced variations in tectonic stress can lead to flow field changes, which have been found as a major cause of engineering accidents and geohazards in practice(Zhu Zhende et al. 2005). Research on development of rock fractures can offer insights into floor rock deformation, damage, and failure as well as geological environments featuring macroscopic coupling. From the perspectives of stress-flow field coupling and engineering practice, the mechanism responsible for fracture development should differ depending on whether there is hydraulic pressure and on the level of confining pressure. Therefore, studying the process of fracture development under varying tectonic stresses, hydraulic pressures and compression rates to determine if fracture development is stochastic or not and the specific mechanism of fracture under the influence of each single factor is of great significance.

Lomize's classical cubic law (Lomize G1951)which deals with the process of water flow in a single fracture, provides a theoretical basis for research on fracture flow. Louis and other scholars (Louis,C et al. 1975)have revised the cubic law through a lot of experiments to

broaden its range of applications. Modern-day technological advancements, especially the combination of computer technology and rock mechanics testing equipment, enable more accurate and comprehensive experimental research into the characteristics of flow in rock in complete stress-strain process. Using electro-hydraulic servo control stiff testing machines, researchers (GAO Yubing et al. 2016)investigated how the permeability of rock under given confining and pore pressures varied with increasing axial compression throughout the process of rock deformation and failure. Other researchers(Purcell W,R et al. 1949) provided systems and methods for flow-creep coupling testing with improved experimental equipment, and experimentally investigated the creep behavior and permeability of rocks that underwent long-term flow-stress coupling. These studies revealed the characteristics of creep failure and the patterns of permeability variation, which provide a basis for research on long-term stability of rock engineering projects. Oda et al.(Oda et al. 2002)analyzed the damage growth in Inada granite and changes in its permeability using the crack tensor concept and conducted transient pulse tests on samples that had been damaged by triaxial compression. The test results demonstrate that permeability tensor can be accurately formulated by microstructural parameters (damage). The results of the analysis suggested that the permeability of the sample subjected to stress high enough to cause failure was 2 to 3 orders of magnitude higher than that of intact granite. All of these studies provide useful references for research into mechanisms responsible for fracture development in floor rocks under the influence of flow-stress coupling.

Analysis of the pattern of stress distribution in a mine floor along the direction of advance of a coal face

Jacobi, a scholar from former West Germany, treated floor strata as a homogeneous elastic body and then simulated and calculated the stress distribution under coal pillars and under coal blocks being extracted. This section describes theoretical calculation of mining-induced stress distribution in a floor along the direction of advance of a coal face using stress increment. Fig. 1 illustrates the distribution of abutment pressure in coal and rock masses along the direction of advance of the face.

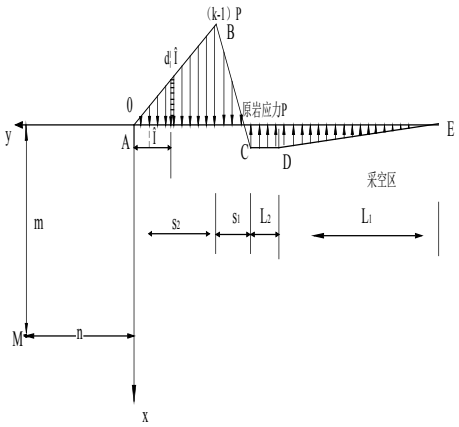

Fig.1 *Distribution state of mining abutment pressure*

Assume that the distribution pattern and level of abutment pressure at the coal face are constant, and the face's position relative to the x-axis remains unchanged, which means that the abutment pressure and the x-axis, moves horizontally along the y-axis as the face advances. Let y denote the distance traveled by the face along the y-axis. The coordinates of M in the new coordinate system are (m-y, n). Eq. (1) can be rewritten as follows:

$$\left.\begin{aligned}\sigma_x &= -\frac{2}{\pi}\int_{y_1}^{y_2}\frac{p(\xi)m^3 d\xi}{\left[m^2+(n-\xi)^2\right]^2}\\ \sigma_y &= -\frac{2}{\pi}\int_{y_1}^{y_2}\frac{p(\xi)m(n-\xi)^2 d\xi}{\left[m^2+(n-\xi)^2\right]^2}\\ \tau_{xy} &= -\frac{2}{\pi}\int_{y_1}^{y_2}\frac{p(\xi)m^2(n-\xi)d\xi}{\left[m^2+(n-\xi)^2\right]^2}\end{aligned}\right\} \quad (1)$$

The results of calculation can be used to determine the three stress components (XXX) resulting from the abutment pressure increment at M (x, 100) as the face moved forward from 140 m behind M to 260 m in front of it. The horizontal line containing point M, given by y=100, was used as the survey line. Eight points were selected from the line, including M1 (40, 100), M2 (35, 100), M3 (30, 100), M4 (25, 100), M5 (20, 100), M6 (15, 100), M7 (10, 100), and M8 (5, 100). The pattern of variation in vertical stress was then derived by substituting the coordinates of these points into Eq. (1) Eq. (1).

According to the results, the stress concentration factors at depths of 5 m, 10 m, 15 m, 20 m, 25 m, 30 m, 35 m, and 40 m in the floor were 2.2, 1.93, 1.73, 1.57, 1.45, 1.35, 1.27, and 1.22, respectively, indicating that the stress concentration factor in the floor decreased with increasing depth. The ratios of vertical stress values at these points to the initial stress were 0.05, 0.1, 0.17, 0.2, 0.24, 0.29, 0.33, and 0.37, respectively, suggesting that the degree of stress relief in the floor decreased with increasing depth of burial.

Permeability of fractured floor rocks

Transient measurement of rock permeability was carried out using the testing system. It is called Electro-Hydraulic Serve controlled Rock Mechanics Testing System, purchased by China University of Mining and Technology from the U.S. instrument manufacturer MTS. The equipment is an advanced rock mechanics testing system for laboratory use. Equipped with three independent closed-loop servo control systems (axial compression, confining pressure, and pore water pressure), it can perform uniaxial (compression) test, pseudo triaxial (compression) test, true triaxial test, pore water pressure measurement, and penetration test. Besides, it can apply loading with different waveforms and at different rates. The vertical compressions on rock and coal samples under test were imposed by the MTS815.02 Electro-Hydraulic Serve controlled Testing System. The displacement and loading rate were kept constant during loading. The sys-

tem was also responsible for collecting real-time data about the vertical loads and deformation experienced by the samples. Fig. 2-4 illustrates how the permeability coefficients of sandstone and mudstone varied with triaxial compression under different confining pressures.

Fig. 2 *Figure of AssemblingPenetrating Equipment*

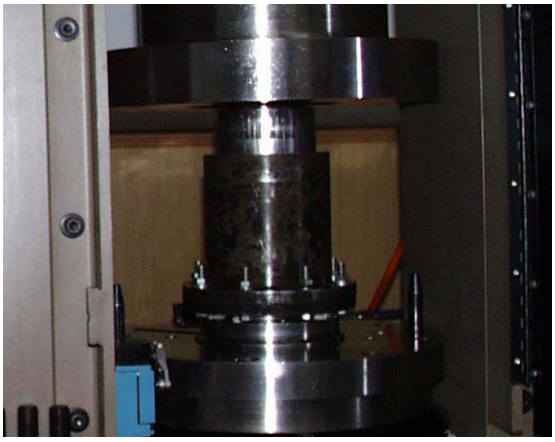

Fig. 3 *Penetrating Equipment Is Working*

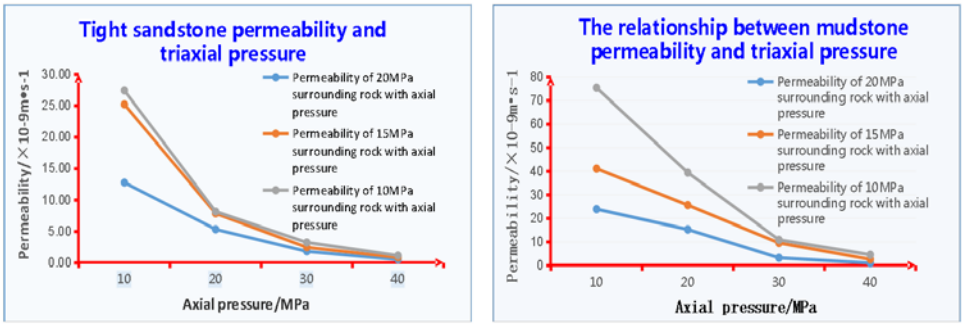

Fig. 4 *Relationship between permeability and triaxial compression for sandstone and mudstone*

Microscopic analysis of permeability of fractured floor rocks using CT scanning

A micro/nano CT scanning test was carried out using nanoVoxel-3502E (Fig. 5), a test system produced by Sanying Precision Motion Control (Tianjin) Technology co., LTD. It has a resolution of 0.5 μm and allows for nondestructive testing. 3D representations of the samples' interior structures were achieved with this system.

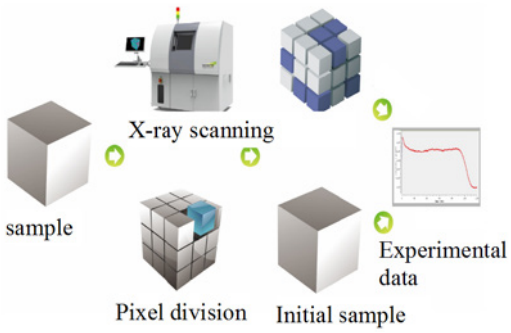

Fig. 5 *Schematic of the test system*

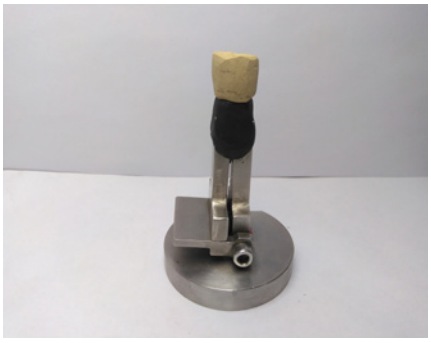

Fig. 6 *Picture of samples*

This section studies the samples taken from the floor strata in a coal mine operated by God Warburg Hiller Energy Corporation based on local geological conditions, with a focus on calculation of the samples' porosities and pore volumes and radii, frequency statistics, and extraction of 3D data such as the numbers of pores and throats, pore-to-throat ratio, and areal porosity. Pores in these samples were quantitatively analyzed using the ball-and-stick theory (Fig. 7).

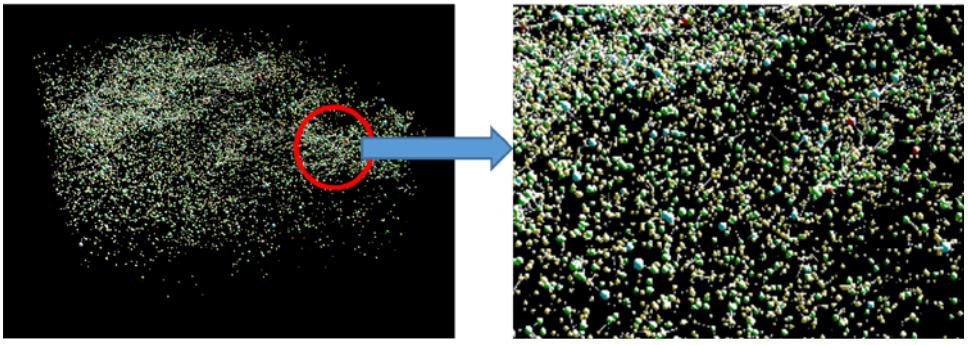

Fig. 7 *Schematic of the ball-and-stick*

In order to study the mechanism of fracture development on a microscopic scale, we planned to first calculate theoretical hydraulic stress, investigate permeability variation with hydraulic stress by rock mechanics testing, and then compare the results with the microscopic permeability under different stress conditions obtained from real-time scanning. However, due to the extra high precision of the instrument, we encountered many difficulties in improving the instrument. The compression equipment was damaged by excess pressure and is now under repair. The research team is currently trying to develop a real-time Nano-CT scan-

ning test scheme that applies to water-rock coupling conditions and can offer resolutions required for industrial CT scanning. Main results achieved are presented to demonstrate our research progress.

The test scheme encompasses the following steps: micro/nano-scale scanning of the sandstone and mudstone samples, soaking the samples in water for four hours, taking them out for scanning again, soaking the sandstone samples in water for 2 hours and scanning them again. It intends to investigate the influence of water on fractures.

Result analysis: Statistics on pores in mudstone before and after soaking.

Table 1 *Statistics on pores in mudstone before and after soaking*

Pore volume interval um^3	Number of pores		Total pore volume um^3	
	Before soaking	After soaking	Before soaking	After soaking
0—2.00×10^4		3876	5.60×10^7	5.40×10^7
2.00×10^4—5.00×10^4	3620	3455	1.28×10^8	1.22×10^8
5.00×10^4—1.00×10^5	3953	3290	2.89×10^8	2.42×10^8
1.00×10^5—5.00×10^5	6629	6522	1.51×10^9	1.50×10^9
5.00×10^5—1.00×10^6	1585	1541	1.11×10^9	1.09×10^9
1.00×10^6—5.00×10^6	1605	1616	3.26×10^9	3.24×10^9
5.00×10^6—1.00×10^7	168	167	1.16×10^9	1.16×10^9
1.00×10^7—5.00×10^7	80	87	1.47×10^9	1.55×10^9
more than 5.00×10^7	7	10	7.72×10^8	1.20×10^9

Table 2 *Statistics on pores in tight sandstone before and after soaking*

		Poro-sity	Total number of pores	Maximum equivalent diameter/um	Average equivalent diameter/um	Maximum pore volume/μm^3	Average pore volume/μm^3
Quantitative analysis of pore size	0h	1.632%	85993	3340.72	88.00	1.95×10^{10}	1.29×10^6
	4h	1.010%	55503	1054.2	87.9	6.13×10^8	9.44×10^5
	6h	0.713%	35109	923.35	94.58	4.12×10^8	1.05×10^6

The analysis reveals that the mudstone's porosity increased with the duration of soaking.

The numbers of small pores, ranging between 0-1.00×106 um3 in volume, decreased after 4 hours of soaking. The numbers of large pores, ranging from 1.00×106 to 5.00×107 um3 in

volume, did not change or increased as the duration of soaking increased. Fractures in the mudstone gradually disappeared during soaking.

The statistics on the sandstone's porosity before and after soaking are presented below. As shown in the figure, after soaking, small pores in the sandstone decreased in both number and total volume, while large pores increased in both number and total volume.

Based on the data from the scanning test, a numerical model was constructed to simulate the flow through it. The permeability coefficient predicted by the model was 15.3×10-9 m•s-1.

Conclusions

The three-dimensional rock stress at a selected position was theoretically calculated. Rock permeability values under different 3D stresses were measured by rock mechanics testing and the patterns of permeability variation with stress were analyzed. After that, micro/nano CT scanning was performed on the rock samples to examine the statistical regularity in pore and throat data and their relationships with the flow through the rocks.

(1) A semi-infinite elastic mechanical model for determining stress distribution in a mine floor was created by additional stress calculation. Triaxial compressions at different locations in the floor were theoretically obtained. The results show that the degree of stress relief decreased as the burial depth increased.

(2) A rock mechanics test was performed on the rock samples using MTS815.02 Electro-Hydraulic Serve controlled Rock Mechanics Testing System. The test results reveal the pattern of permeability variation with and the ratio of confining pressure to axial compression.

(3) 3D representations of test samples' interior structures were realized by micro/nano CT scanning. Quantitative analysis and space inversion of pores within the samples were performed using the ball-and-stick theory.

Acknowledgements

Financial supports from the State Key Research Development Program of China (2016YFC0501100) and Natural Science Funds Project (Grant No.51604007) are greatly appreciated.

References

Zhang Youtian (2005) Rock Hydraulic Engineering and Engineering. China Water Conservancy and Hydropower Press, Beijing,482pp

Zheng Shaohe,Yao Hailin,Ge Xiurun (2004) Coupling analysis on seepage and damage in fractured rock mass. Chinese Journal of Rock Mechanics and Engineering 09:1413-1418.

WANG Xi-liang,PENG Su-ping,ZHENG Shi-shu (2004) Controlling and predicting water inrush with high pressure in deep mining.Journal of Liaoning Technical University 06:758-760.

Zhu Zhende,Sun Jun (1999) Coupled Analysis Model of Seepage Field and Damage Field in Fractured Rock Mass and Its Engineering Application. journal of yangtze river scientific research institute 05:22-27.

YANG Tianhong,TANG Chun-an,TAN Zhihong,ZHU Wancheng,FENG Qiyan (2007) State of The Art of Inrush Models in Rock Mass Failure and Developing Trend for Ediction and Forecast of Groundwater Inrush. Chinese Journal of Rock Mechanics and Engineering 02: 268-277.

Lomize, G (1951) Flow in fractured rocks. Gosenergoizdat, Moscow, 1951, 127.

Louis,C (1975) Rock hydraulics:Report. BRGM, ORLEANS, FRANCE, NO. 74 SGN 035 AME, 1974 International Journal of Rock Mechanics and Mining Sciences & Geomechanics Abstracts 12(2): 59.

Jones Jr, F. A laboratory study of the effects of confining pressure on fracture flow and storage capacity in carbonate rocks[J]. Journal of Petroleum Technology 27(1): 21-27.

GAO Yubing,LIU Shiqi,LYU Bin,LI Kunqi (2016) Mechanism study of floor water inrush around mining field based on micro-crack extension Journal of Mining & Safety Engineering 04:624-629.

Wang Yong – hong, Shen Wen (1996) Prevention and Control of Water Hazards in Coal Mines in China[M].Beijing:Coal Industry Press. 366pp

Chen Zhanqing, Yu Bangyong (2015) Advances in seepage mechanics of mining rock mass[J].Journal of Southwest Petroleum University (Natural Science Edition) 03:69-76.

Purcell W R (1949) Capillary pressures—Their measurement using mercury and the calculation of permeability therefrom. Journal of Petro-leum Technology 1(2):39-48.

Thomeer J H M (1960) Introduction of a pore geometrical factor defined by the capillary pressure curve. Journal of Petroleum Technology 12(3):73-77.

Oda,M.,Katsube,T.,Takemura,T (2002) Microcrack evolution and brittle failure of Inada granite in triaxial compression tests at 140 MPa . Journal of Geophysical Research 107(B10).